

Low frequency radio monitoring of Cygnus X-1 and Cygnus X-3

M. Pandey¹, A. P. Rao², G. G. Pooley³, P. Durouchoux⁴, R. K. Manchanda⁵, C. H. Ishwara-Chandra²

¹ Dept. of Physics, Mumbai University, Mumbai - 400 098, India

² NCRA, TIFR, Post Bag 3, Ganeshkhind, Pune - 411 007, India

³ Cavendish Laboratory, University of Cambridge, Madingley Road, Cambridge CB3 0HE, UK

⁴ CNRS FRE 2591/CEA Saclay, DSM/DAPNIA/SAP, F-91191 Gif sur Yvette Cedex, France

⁵ Tata Institute of Fundamental Research, Mumbai-400005, India

⁶

Received ; accepted

Abstract. We present results of monitoring observations of the micro-quasars Cygnus X-1 and Cygnus X-3 at 0.61 and 1.28 GHz. The observations were performed with Giant Meter-wave Radio Telescope, GMRT, between 2003 June and 2005 January. Variable, unresolved sources were found in both cases. Cyg X-1 was detected in about half of the observations, with a median flux density about 7 mJy at each frequency. The results show clearly that there is a break in the spectrum above 1.28 GHz. The variations in Cyg X-1 may be due to refractive interstellar scintillation. Cyg X-3 was detected in each observation, and varied by a factor of 4. For this source, models of the scintillation suggest a very long timescale (of the order of 40 yr at 1.28 GHz), and therefore we believe that the variations are intrinsic to the source.

Key words. binaries : close – stars : individual : Cygnus X-1, Cygnus X-3 – ISM : jets and outflows – radio continuum : stars

1. Introduction

The X-ray sources Cygnus X-1 and Cygnus X-3 are accreting X-ray binary systems which have been classified as micro-quasars. The X-ray emission in such systems is believed to originate in the inverse Comptonization of seed photons in the accretion disc; the sources exhibit several spectral states classified as low-hard, intermediate and high-soft state (Cui 1999). The spectral analysis of the radio emission from these X-ray binaries with black hole candidates (BHCs) suggests that the radio emission arises due to synchrotron emission from the high energy electrons emitted in the jets (Hjellming & Johnston 1988; Hjellming & Han 1995) and the radio emission is quenched when a source is in high-soft X-ray state (Corbel et al. 2000), and detected in both low-hard and intermediate X-ray state. High-resolution mapping of X-ray binaries, particularly the well-known object GRS 1915+105, has demonstrated the presence of relativistic outflows (hence the term ‘micro-quasars’). Such motions have been mapped in Cyg X-3 (Mioduszewski et al 2001), and a jet-like feature has been mapped in Cyg X-1 (Stirling et al 2001). There has been a variety of other studies, mostly at high

radio frequencies (above 2 GHz). However, the low frequency characteristics of Cyg X-1 in particular have not been explored so far.

To understand the physical mechanism connecting the inflow and outflow of matter in such systems, a comprehensive study of the correlation between radio and X-ray emission in different states of these sources is necessary. We have carried out systematic monitoring of micro-quasars using the Giant Meter-wave Radio Telescope, GMRT (Pandey et al. 2004) at low frequencies. In this paper, we present the observations of Cyg X-1 and Cyg X-3, which demonstrate variations in the flux densities at low radio frequencies for both these sources. The observed flux density variations can be ascribed either to intrinsic mechanisms specific to each source, i.e. a process occurring around the compact sources themselves, or to refractive interstellar scintillation. The refractive scintillation can be described as the flux density variations caused by “focusing” and “defocusing” of electromagnetic waves by large scale plasma density irregularities in the interstellar medium (Rickett et al. 1984).

2. Observations and Analysis

The radio snapshot observations (of duration 30 min) were carried out at 0.61 GHz and 1.28 GHz with a bandwidth of 16/32 MHz using the Giant Meter-wave Radio Telescope, GMRT. The flux density scale was set by observing the primary calibrators 3C286 and 3C48. Phase calibrators were interleaved with 25 min scans on each of Cyg X-1 and Cyg X-3. The sampling time was 16 s. The data recorded from GMRT was converted into FITS files and analyzed using the Astronomical Image Processing System (AIPS). A self calibration on the data was used to correct for phase related errors and improve the image quality. Tables 1 and 2 summarize details of observations using GMRT at the two frequencies between June 2003 and Jan 2005. Cyg X-3 was detected in each observation and Cyg X-1 during about one-half of them. Columns 1, 2 and 3 in both the tables gives the dates of observations and the measured flux densities or upper limits. Column 4 gives the corresponding rms noise in the field of the radio image. For the observations performed during telescope maintenance/test time the background noise was higher because of the reduced number of antennas available. For each field there are some 6 background sources detected. We record in Tables 1 and 2 the measured flux density of one from each field, at an angular distance of 15' (Cyg X-1) and 22' (Cyg X-3). The measured flux densities of these 'control' sources are consistent with constant actual flux densities and the observed noise levels. This result gives us overall confidence in the reliability of the system.

To supplement the data from GMRT, we have also used radio data on Cyg X-1 and Cyg X-3 taken with the Ryle Telescope at 15 GHz. The longitudes of the GMRT and Ryle Telescope differ by 74 deg (5 hr), and so the observations are usually not exactly simultaneous; in the worst cases the nearest 15-GHz observation is separated by 2 days from the GMRT observation. The radio light curve at 15 GHz for Cyg X-1 was averaged for 10 min, that for Cyg X-3 for 5 min. The typical uncertainty is 2 mJy + 3% in the flux scaling. In column 6 of the Tables we have listed the flux density at 15 GHz for the nearest observation at that frequency. Column 7 gives the spectral indices between the GMRT observation and 15 GHz (in the sense $S \propto \nu^\alpha$). Column 8 gives the X-ray spectral state of the source as determined from the 2-12 keV light curves of the sources taken from the ASM archival data.

In Fig. 1 and Fig. 2 we show the first ever radio images of Cyg X-1 and Cyg X-3 at 0.61 GHz. The AIPS subroutine `jmfit` shows that the images are consistent with point sources.

3. Discussion

3.1. Cyg X-1

Cyg X-1 is bright X-ray source with a mass in excess of $7M_\odot$ (Gies & Bolton 1986) and a distance of ~ 2.5 kpc. The companion is an O9.7Iab super-giant (V1357 Cyg, HDE 226868), showing a strong stellar wind (Persi et al.

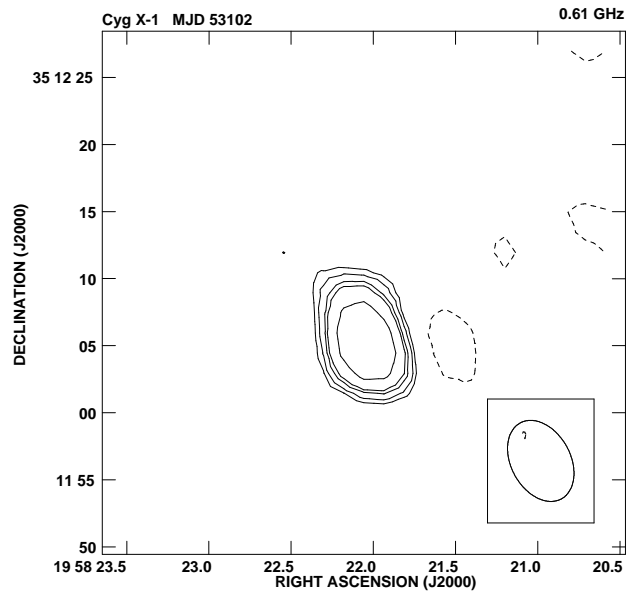


Fig. 1. GMRT image of Cyg X-1. The contour levels are $1.3\text{mJy} \times (-1, 1, 1.4, 2, 4, 8)$.

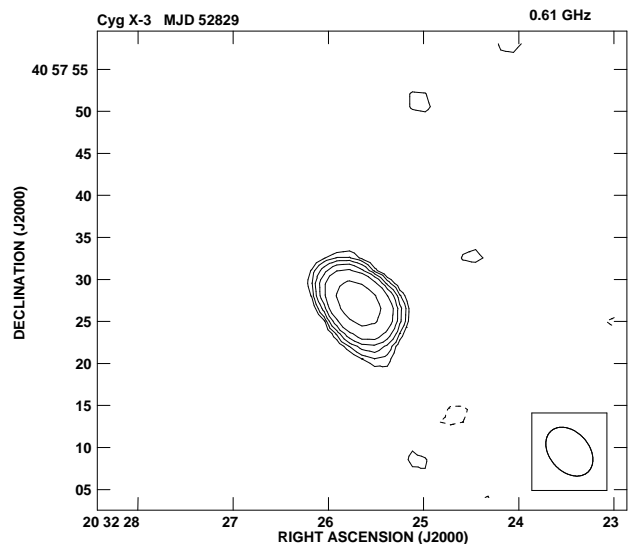


Fig. 2. GMRT image of Cyg X-3. The contour levels are $2.3\text{mJy} \times (-1, 1, 1.4, 2, 4, 8)$.

1980) and almost filling its Roche lobe (Bolton 1972). The observed radial velocity for the system $v \sin i$ is about 76 km s^{-1} (Gies & Bolton 1982). The emission in X-rays and in the radio band vary over a wide range of time-scales, including modulation at the 5^d.6 orbital period; see, for example, Brocksopp et al (1999) and Gleissner et al (2003). The X-ray emission is usually in the spectral state described as 'low-hard' (with a non-thermal com-

Table 1. Flux density of Cyg X-1 between 2003 Jun and 2005 Jan

Date MJD ν /GHz	S_ν (mJy)		GMRT rms noise (mJy)	Control Source (mJy)		S_ν (mJy)	α	X-ray state
	0.6	1.2		0.6	1.2			
	0.6	1.2		0.6	1.2			
52796	-	≤ 4.8	1.6	-	4.2	13	≥ 0.6	H-S
52799	-	10.1	1.3	-	5.2	22	0.3	H-S
52827	≤ 2	-	0.5	9.1	-	8	≥ 0.4	H-S
52829	≤ 1.5	-	0.4	8.9	-	13	≥ 0.5	H-S
52845	-	≤ 7	2.2	-	4.7	6	≥ 0.06	H-S
52848	-	≤ 5	1.3	-	4.8	6	≥ 0.07	H-S
52855	-	5.4	0.2	-	5.7	22	0.8	Int
52891	5.8	-	0.7	9.2	-	15	0.3	L-H
53037	-	9.2	0.2	-	4.4	15	0.2	Int
53102	9.7	-	0.4	10.3	-	22	0.3	L-H
53104	≤ 7	-	2.0	8.9	-	27	≥ 0.4	L-H
53107	10.3	-	0.7	10.3	-	26	0.3	L-H
53127	≤ 7	-	2.1	10.5	-	16	≥ 0.3	L-H
53377	≤ 5.1	-	1.7	8.7	-	6	≥ 0.05	H-S
53379	≤ 3.3	-	1.1	8.5	-	6	≥ 0.2	H-S
53391	8.4	-	0.9	9.5	-	20	0.3	Int
53392	8.4	-	0.8	9.3	-	16	0.2	Int

Table 2. Flux density of Cyg X-3 between 2003 Jun and 2005 Jan

Date MJD ν /GHz	S_ν (mJy)		GMRT rms noise (mJy)	Control Source (mJy)		S_ν (mJy)	α	X-ray state
	0.6	1.2		0.6	1.2			
	0.6	1.2		0.6	1.2			
52797	-	57.9	0.4	-	7.7	70	0.08	L-H
52800	-	90.4	0.5	-	9.6	110	0.08	L-H
52830	31.2	-	0.8	16.6	-	115	0.4	L-H
52849	-	62.4	0.4	-	9.4	190	0.5	L-H
52856	-	53.5	0.3	-	8.4	132	0.4	L-H
52892	7.0	-	0.7	17.8	-	73	0.7	L-H
53037	-	21.2	0.3	-	8.1	51	0.4	L-H
53105	14.5	-	1.1	16.6	-	45	0.4	L-H
53107	13.0	-	0.8	20.1	-	70	0.5	L-H
53127	40.8	-	1.1	18.6	-	50	0.06	L-H
53128	29.5	-	0.8	19.5	-	73	0.3	L-H
53378	31.4	-	1.7	18.7	-	130	0.4	H-S
53379	29.8	-	1.1	18.5	-	130	0.5	H-S
53392	27.3	-	0.9	19.5	-	170	0.6	H-S
53393	44.2	-	0.8	19.3	-	170	0.4	H-S

ponent extending to a few hundred keV); the relatively rare ‘high-soft’ state is dominated by a strong low-energy component. The high-frequency radio emission tends to be suppressed during the high-soft states (Hjellming, Gibson & Owen 1975) (see Fig. 4). While the X-ray source is in the low hard state, the radio emission in the cm-wave band is persistent, but the magnitude does vary by a factor of about 5, with very rare outbursts to higher flux densities. These variations are much less spectacular than those of some other members of this class such as Cyg X-3 and GRS 1915+105. The radio spectral index α , defined in the sense $S \propto \nu^\alpha$, is close to zero in the range 2 – 220 GHz (Fender et al 2000). Jet emission in Cyg X-1 has also been observed at milliarcsec resolution during the low-hard state at 8.4 GHz (Stirling et al. 2001). This jet is also not as dramatic (in terms of rapid vari-

ability and relativistic outflows) as in the cases of jets observed in a number of other microquasars e.g. Cyg X-3 (Miouduszkeski et al 2001), GRS 1915+105 (Dhawan et al. 2000), IE 1740.7–2942 (Mirabel et al. 1992), and GRS 1758-258 (Rodríguez et al. 1992). Observations by Gallo et al (2005), however, suggest that the jet may be inflating a large (5 pc) shell-like structure around the X-ray source, implying that its contribution to the outflow of energy in this system is dominant. Fig. 3 shows the low-frequency flux density from GMRT plotted against the closest available 15-GHz flux density. Different markers are used for the two GMRT frequencies. There is a clear correlation between the high- and low-frequency data, somewhat complicated by the upper limits on some of the GMRT flux densities, but nevertheless convincing.

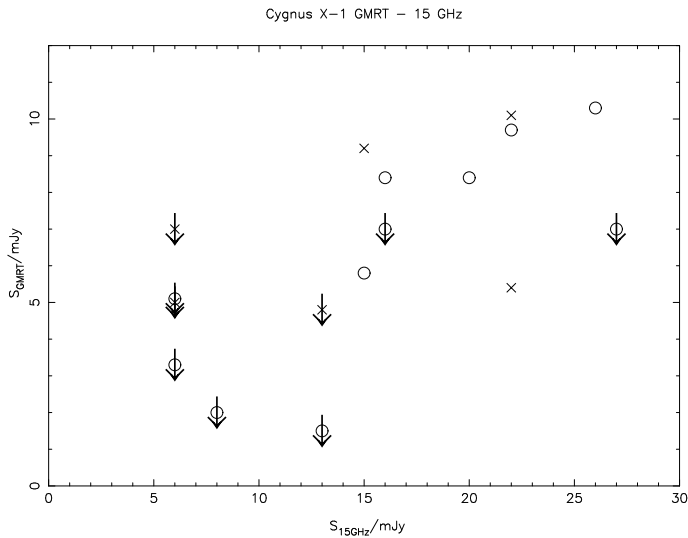


Fig. 3. Flux–flux plot for Cyg X-1 showing the low-frequency GMRT flux densities (\circ 0.61 GHz, \times 1.28 GHz) and the closest 15-GHz measurement.

3.1.1. The radio and X-ray association of Cyg X-1

The 15-GHz radio light curve and the RXTE/ASM X-ray count-rate and hardness ratio HR2 for Cyg X-1 from 2003 Mar to 2005 Jan are shown in Fig.4 (daily averages for both of the X-ray parameters are used). The X-ray state of the system changed several times over this interval. For the majority of the time, Cyg X-1 was in the low-hard state, but with three distinct periods of the high-soft state lasting 1 – 2 months each. The suppression of the 15-GHz flux density during the high-soft states is well-illustrated by these data.

There was one exceptional flare recorded in the 15-GHz data, on 2004 Feb 20.27, where the flux density reached a maximum of 140 mJy in an event which lasted about 30 min. Unfortunately there was no GMRT observation at this date.

3.1.2. Spectral and temporal behaviour of Cyg X-1

Cyg X-1 is a persistent but variable flat-spectrum source over the range 2 to 220 GHz (Fender et al. 2000). It is clear from table 1 and Fig. 3 that Cyg X-1 was detected at low frequency in only one of the 8 observations while it was in the high-soft X-ray state. Observations in the intermediate and low-hard X-ray states all resulted in detections, apart from two which both had relatively high noise levels. Therefore we conclude that the high-soft state suppresses the radio emission at low radio frequencies as it does at high frequencies. There is no clear distinction between the radio spectral index of the intermediate and low-hard states, being typically $\alpha = 0.3$. While all of these spectral measurements are subject to the additional uncertainty from the lack of precisely simultaneous observations, we also conclude that the radio spectrum rises from

the GMRT observing frequencies to the regime where it is essentially flat (2 to 220 GHz). Part of the variation of radio emission from Cyg X-1 is associated with the X-ray state of the system, and is therefore intrinsic. A further part may be associated with propagation through the interstellar medium – in particular, refractive interstellar scintillation (RISS) may introduce amplitude variations (Rickett, 1990). We have used the NE2001 code made available by Cordes & Lazio (1993) to estimate the propagation parameters for Cyg X-1 and Cyg X-3.

The NE2001 code estimates that the transition frequency (above which the scattering is weak, and therefore the intensity fluctuations small) is around 6 GHz. The angular broadening is estimated as 0.3 mas at 0.61 GHz and 0.06 mas at 1.28 GHz. The scattering disc is therefore about 1×10^{11} m at 0.61 GHz and 2×10^{10} m at 1.28 GHz. If we assume that typical transverse velocities involved (the source or the medium) are near 100 km s^{-1} , we derive timescales of 5 and 1 days at the two frequencies. These are clearly in the same area as those of the observed fluctuations, so it is quite possible that RISS is a contributing factor. We note, however, two further points. The angular size of the (transient) radio jet mapped at 8.4 GHz by Stirling et al. (2001) is 10 mas: the low-frequency emission may originate in a region of this size (or larger); and the scintillation bandwidths estimated by the NE2001 code are 30 and 100 MHz at 0.61, 1.28 GHz. Both of these would reduce the observed RISS contribution to the fluctuations.

3.1.3. Proposed geometry and emission mechanism

From the above discussion, we conclude that the radio spectrum of Cyg X-1 consists of two parts, the persistent high frequency emitting component and the variable low frequency component. Both of these components imply the presence of a continuous jet with discrete plasmoids or clouds of electrons, emitting synchrotron photons. The observed behaviour of the source at radio frequencies can be explained by adiabatically expanding plasmoids in conical jets (Hjellming et al. 1988), where the low frequency radio emitting component is significantly altered by refractive interstellar scintillation giving rise to high variability in the radio flux density. A sketch of the proposed geometry is shown in Fig. 5. In our model compact plasmoids are ejected continuously at the base of the jet and expand freely outward. The low frequency emission from the newly ejected plasmoids will be absorbed due to synchrotron self absorption in an optically thick medium because of its highly compact nature and high magnetic field. The plasmoid will be still visible at high radio frequencies (Miller-Jones et al. 2004). As the plasma expands under its internal pressure, it will become optically thin and emit over the whole radio-frequency band, although at a lower intensity.

The observed flat radio spectrum of Cyg X-1 can thus be explained as due to superposition of individual self-absorbed synchrotron components emitted or plasmoids

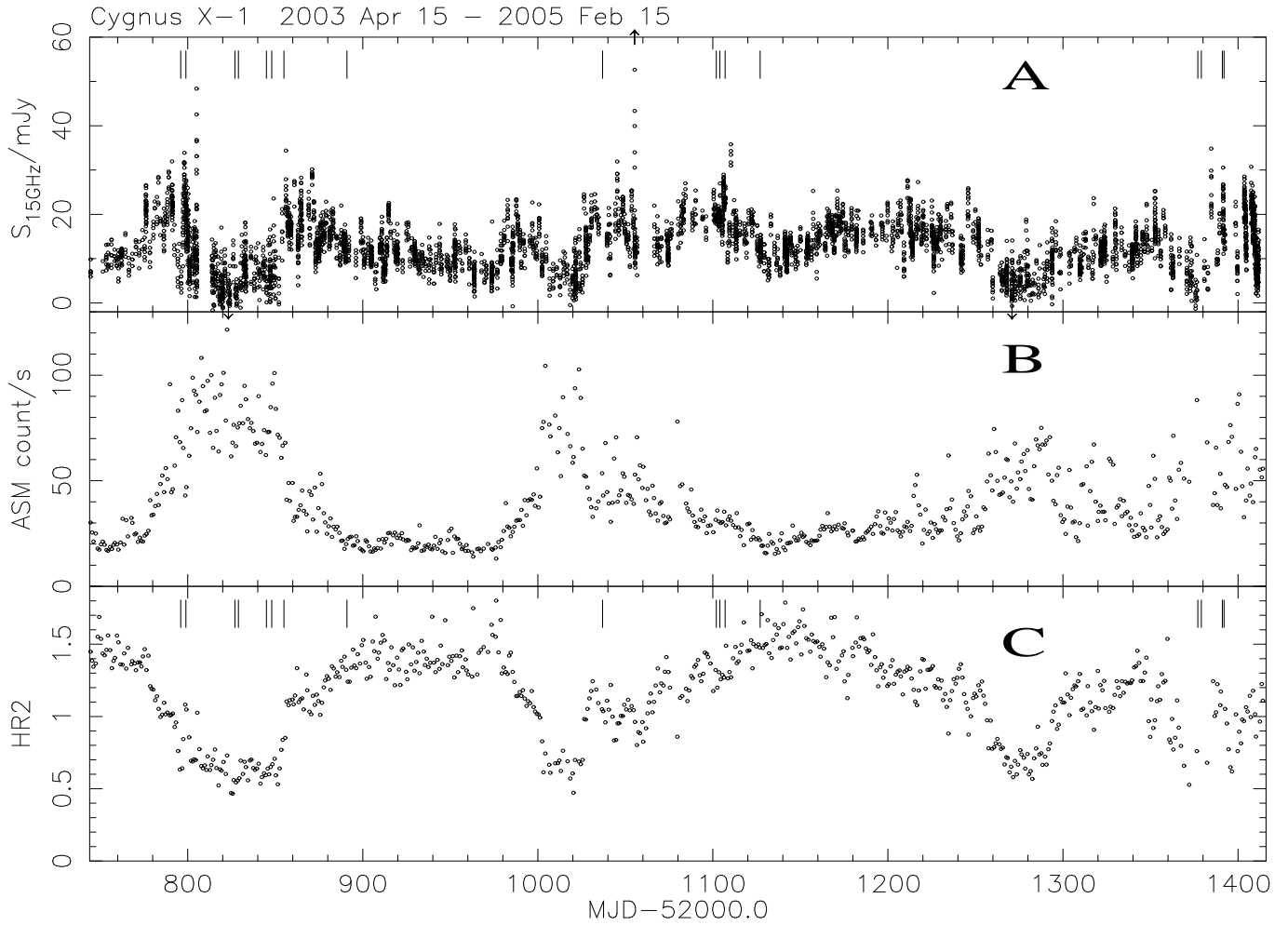


Fig. 4. Cygnus X-1: Radio (15 GHz) (top) and RXTE/ASM (middle) light-curves; ASM hardness ratio $HR2=(5-12)\text{keV}/(3-5)\text{keV}$ (bottom) during the interval $MJD\ 52796 = 2003\ \text{Jun}\ 06$ to $MJD\ 53392 = 2005\ \text{Jan}\ 22$. The dates of GMRT observations are marked with vertical lines.

with differing age profile and having longer life time. If a combination of size and the magnetic field are such that opacity effects are important only for the younger population, an inverted (or overall flat) spectrum is seen. The average spectrum can also mimic a flux level shift above a cut-off frequency, characterized by the optical thickness of the medium and the choice of age distribution. As discussed earlier, the 15-GHz and GMRT flux densities are correlated; while we do not believe that the 15-GHz data are significantly affected by scintillation, this may not be the case at the GMRT frequencies and at least some of the variance in the 0.61 and 1.28 GHz data results from RISS. In conclusion, the radio emission in Cyg X-1 is mainly due to a continuous outflow of compact plasmoids or electron clouds into a jet and the spectrum consists of the composite emission from each of these slow decaying ejecta and mini flaring events as observed in the source may result due to randomness of the age distribution of the ejected clouds.

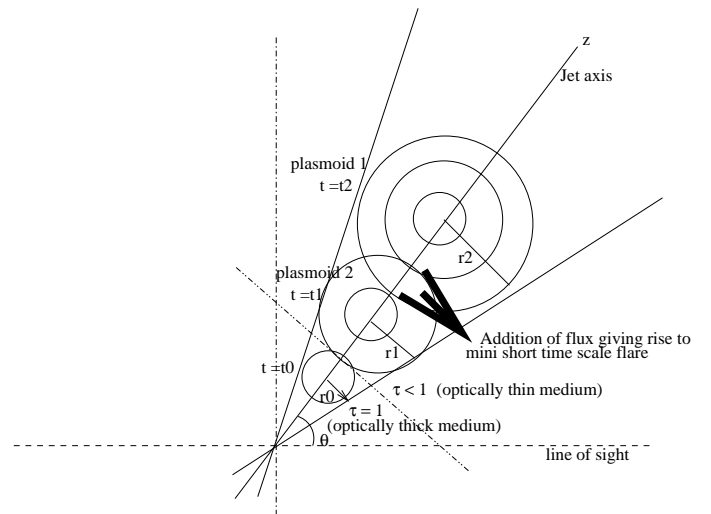


Fig. 5. Model for Cyg X-1 jet

3.2. Cyg X-3

Cyg X-3 is an X-ray binary system which does not seem to fit easily into the established classes of these systems. It is probably a low mass X-ray binary system. It has a 4.8-hr orbital period, and is located in the Galactic plane at a distance of ~ 10 kpc (Predehl et al. 2002; Dickey 1983; Mason et al. 1979). The optical counterpart of the X-ray source is a WR star (van Kerkwijk et al. 1996), which is not visible in the optical band because of heavy interstellar extinction but is clearly seen above $\sim 0.8\mu\text{m}$. The optical data also shows a 4.8-hr modulation corresponding to the orbital period as seen in X-rays (Hanson et al. 1999). The source exhibits two spectral states low-hard and high-soft similar to Cyg X-1 and has been observed up to 500 keV during the flare mode. The quasi-periodic oscillations with periods between 50 – 1500 s are the key characteristics of the source (van der Klis & Janson 1985). A detailed analysis of the X-ray spectrum suggests that the total no of X-ray photons seems to be conserved at all times irrespective of the state and the observed spectrum is consistent with a thermal source embedded in a hot plasma and enveloped in a cold hydrogen shell (Manchanda 2002). The X-ray light curve of the source in the 2-12 keV band from the RXTE/ASM data shows frequent spectral changes between the high-soft to low-hard states thereby suggesting large changes in the accretion rate on to the compact object.

At radio wavelengths, Cyg X-3 is the most luminous X-ray binary in both its quiescent and flaring states (Waltman et al. 1995). Huge radio outbursts have been reported in Cyg X-3 during which the flux density can increase up to levels of ~ 20 Jy; radio emission is suppressed (“quenched”) to levels below 1 mJy for some days before large radio flares (Waltman et al. 1994). Jet-like structures with repeated relativistic ejection have been observed at various radio frequencies (e.g. Schalinski et al. 1998). On an arc-second scale, two-sided jets have been seen from the source in the N-S orientation, whereas a highly-relativistic ($\beta \geq 0.81$) one-sided jet with the same orientation has been reported on milli-arcsec scales with the VLBA (Martí et al. 2001; Mioduszewski et al. 2001).

3.2.1. Temporal characteristics in the radio band and their association with the X-ray emission

In the Table 2 above we have summarized the radio flux densities of the source as measured during various observations with GMRT and from the Ryle Telescope data. Fig. 6 shows a flux–flux plot for Cyg X-3 for the GMRT and 15-GHz data, and Fig. 7 shows the 15-GHz and RXTE ASM data for the whole period. The timing of the GMRT observations is again marked with vertical lines in Fig. 7. The last 4 GMRT observations, all at 0.61 GHz, were made during the high-soft state. The mean flux density at that frequency was 33.2 mJy, compared with 22.7 mJy for the 6 previous data points; the 15-GHz mean value was also higher, 150 mJy compared with 71 mJy for the cor-

responding 6 data points. We note that the radio/X-ray correlation is in the opposite sense to that for Cyg X-1. McCollough et al (1999) report both anti-correlations (in the quiescent state) and correlations (in the flaring state) between the hard X-ray flux (20–100 keV, as measured by BATSE) and the cm-wave radio flux density of Cyg X3.

We investigated the possibility that RISS might be important in the case of Cyg X3. The propagation conditions are more severe than for the case of Cyg X-1: the path length is much longer, and it has been known for some time (e.g. Wilkinson et al, 1994) that the scatter-broadening for this source is extreme. The NE2001 model is consistent: it suggests angular broadening of 20.59, 4.03 arcsec at 0.61, 1.28 GHz. The corresponding timescales would be many years, and the narrow scintillation bandwidth (2 Hz) would suppress any observed scintillation. We conclude that RISS is not relevant to this study of Cyg X-3.

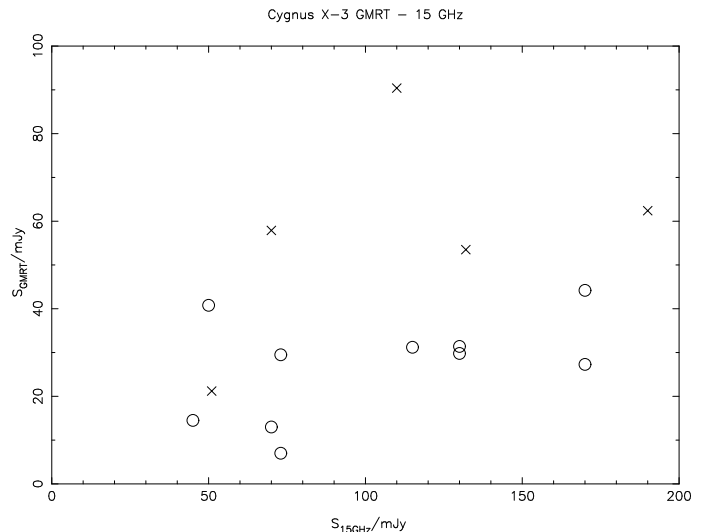


Fig. 6. Flux–flux plot for Cyg X-3 showing the low-frequency GMRT flux densities (\circ 0.61 GHz, \times 1.28 GHz) and the closest 15-GHz measurement

To look for correlation between the radio emission from the source with its X-ray emission characteristics, we have plotted the RXTE/ASM X-ray light curve for Cyg X-3 in Fig. 7 along with the radio data. The timing of the GMRT observations is shown by the vertical lines. It can be seen that no large flares were observed during this interval. The radio emission is in the ‘quiescent’ state, typically 50 to 200 mJy at 15 GHz. For the last month or so of this time-range, the X-ray spectrum softens: the RXTE ASM ratio HR2 falls consistently below 2, and the radio emission starts to become more erratic. This behaviour faded away after another month or so, and the source returned to the quiescent state.

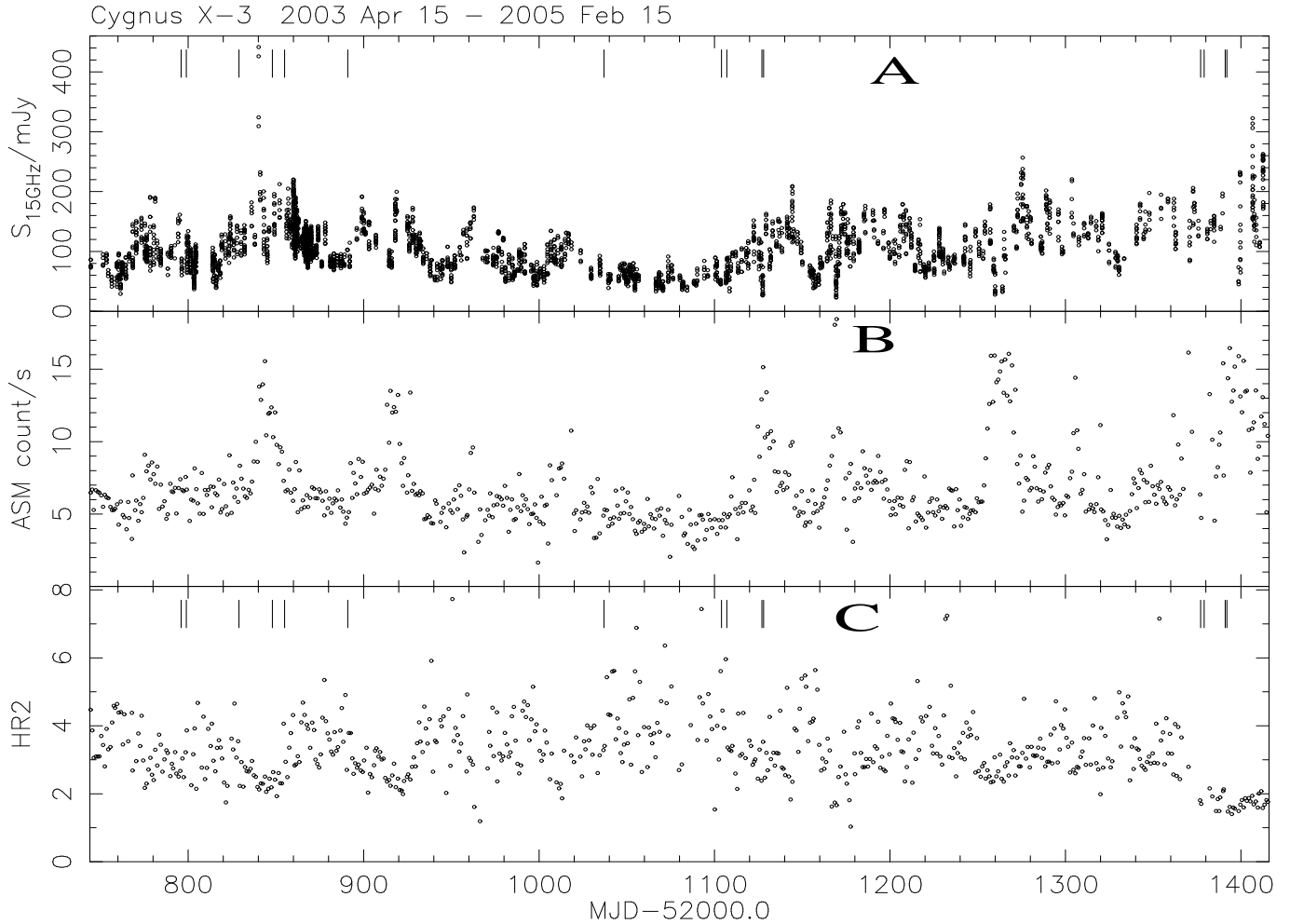


Fig. 7. Cygnus X-3: Radio (15 GHz) (top) and RXTE/ASM (middle) light-curves; ASM hardness ratio (bottom), $HR2=(5-12)\text{keV}/(3-5)\text{keV}$ during the interval MJD 52796 = 2003 Jun 06 to MJD 53392 = 2005 Jan 22. The dates of GMRT observations are marked with vertical lines.

3.2.2. Spectral behaviour and the emission geometry

As seen from the data in Table 2 and Fig. 6, Cyg X-3 is a persistent radio source at all wavelengths. Cyg X-3 is more luminous at higher frequencies. The data in Table 2 clearly indicates a low frequency turn-over in the source spectrum below 1 GHz. As discussed earlier, such behaviour can arise due to synchrotron self absorption of the compact radio emitting plasma in an optically thick medium. The observed variability of the flux density is consistent with the assumption of a discrete ejection/plasmoid in adiabatic expansion. The ejection rate and/or lifetimes of plasmoids in Cyg X-3 are probably lower/shorter than in Cyg X-1 with little or no overlap of the spectra associated to the single discrete ejections. The spectrum and the fact that the radio emission is persistently at an high level may therefore imply an uninterrupted low-rate ejection.

4. Summary

In this paper we have presented the first ever low frequency maps of Cyg X-1 and Cyg X-3 along with the tem-

poral behaviour from the monitoring observations of these sources over two years at various frequencies. It was noted that while Cyg X-3 is persistent source at low frequencies, Cyg X-1 is transient in nature with mean radio flux being 7 mJy and the source is detected at low radio frequencies only when the high frequency radio flux crosses the mean threshold of 15 mJy. The spectral characteristics of both sources too have many similarities e.g. the spectral turn over at lower frequencies. Continuous blob of plasmoids are emitted within the jet medium in both the cases. However the life time of the individual blob in the case of Cyg X-1 is larger than in the case of Cyg X-3 and hence a flatness in the radio spectra is seen in the case of Cyg X-1. The positive detection of Cyg X-1 at 0.61 to 1.2 GHz on several occasions along with the spectral turnover at low frequencies conclusively support the synchrotron origin of the radio photons contrary to its ambiguous thermal or non-thermal nature concluded from earlier measurements (Fender et al. 2000). In the case of Cyg X-3, a close correlation is seen in the change of X-ray hardness ratio and the

radio flux densities during the flaring and quiescent stages thus providing a consistent picture of disc-jet connection.

Rigorous calculations were performed to look for the effect of refractive interstellar scintillation at low frequency on the data of these two sources. The present data clearly indicate that the source visibility above a threshold luminosity seen in Cyg X-1 is due to this effect. However the variability at high frequencies is intrinsic to the source and least affected by interstellar scintillations. Finally, we have discussed a common jet emission model for both the sources in which synchrotron radiation-emitting plasmoids originate at the base of the conical jet and the observed spectral features are due to the superposition of many such plasmoids with different age profile. Thus detailed spectral measurements in the m-cm regime (low frequency radio) combined with simultaneous X-ray data can provide a clear understanding of the emission mechanisms in these sources.

Acknowledgements. We wish to thank the help received from the GMRT staff during the observations. MP wishes to thank NCRA for providing hospitality to carry on this work and acknowledges the financial support received from Raman Research Institute Trust, Bangalore during the early part of this work. She is also thankful to Prof. V. Kulkarni from Mumbai Univ. for constant encouragement. Part of the work is supported by the Indian Space Research Organization grant under the REPOOND program. The RXTE ASM quick-look results provided by the ASM/RXTE team are gratefully acknowledged. The Ryle Telescope is supported by PPARC.

References

- Bolton, C., 1972, *Nature*, 240, 124
 Braes, L. & Miley, G., 1971, *Nature*, 232, 246
 Belloni, T., Klein-Wolt, M., Mendez, M. et al. 2000, *A&A*, 355, 271
 Blandford, R. D., 1989, *Theory of accretion Disks* ed. P. Meyer, W. Duschl, J. Frank, E. Meyer-Hofmeister (Dordrecht: Kluwer), 35
 Brocksopp, C. et al 1999, *MNRAS*, 309, 1063
 Coles, W. A., Frehlich R., Rickett B., et al. 1987, *ApJ*, 315, 666
 Cordes, J. M., Chatterjee, S., Lazio, T., 2003, *ASPC*, 302, 225
 Cordes, J. M., Lazio T., 2003 *The Cordes-Lazio NE2001 Galactic Free Electron Density Model*, http://rsd-www.nrl.navy.mil/7213/lazio/ne_model/
 Cordes, J. M., Lazio T., 2004, *ASPC*, 317, 211
 Corbel, S., Fender, R. P., Tzioumis, A. K., et al. 2000, *A&A*, 359, 251
 Cui, W., 1999, 'High Energy Processes in Accreting Black Holes' ed. J. Poutanen & R. Svensson, (San Francisco: Astron Soc Pacific), p.97
 Dhawan, V., Mirabel, I. F., Rodríguez, L. F., 2000, *ApJ*, 543, 373
 Dickey, J., 1983, *ApJ*, 273L, 71
 Fender, R. P., Pooley, G. G., Durouchoux, P. et al. 2000, *MNRAS*, 312, 853
 Gallo, E., et al. 2005, *Nature* 436, 819
 Gies D., Bolton C., 1982, *ApJ*, 260, 240
 Gies D., Bolton C., 1986, *ApJ*, 304, 371
 Gierlinski, M., Zdziarski, A., et al. 1977, *MNRAS*, 288, 958
 Gleissner, T. et al, 2004, *A&A*, 425, 1061
 Hanson, M. M., Still, M. D., Fender, R. P., 1999, *AAS*, 195, 3906
 Hjellming, R., Gibson, D., Owen, F., et al. 1975, *Nature*, 256, 111
 Hjellming, R., Han, X., 1995, 'X-ray Binaries', ed W.H.G.Lewin, J. Van Paradijs & E.P.J. van den Heuvel (Cambridge: Cambridge University Press)
 Hjellming, R., Johnston J., 1988, *ApJ*, 328, 600
 Ishwar-Chandra, C., Rao, A. P., Pandey, M. D., et al, 2004, *Proceedings of 5th Micro-quasar workshop*, Chinese Journal of Astro. & Astrophys
 Konigl, A., 1989 *ApJ* 342, 208
 Konigl, A., Ruden, S. P., 1992 *Protostars and Planets III*, ed. E.H. Levy & J. I. Lunine (Univ. of Arizona Press)
 Levine, A. M., Cui, W., Remillard, R., et al. 1996, *AAS*, 189, 3511
 Mason, K. O., Sanford, P. W., 1979, *MNRAS*, 189P, 9
 Martí, J., Paredes, J. M., Peracaula, M., 2001, *A&A*, 375, 476
 Manchanda, R. K., 2002, *J. Astrophys. Astr.*, 23, 197
 McCollough, M.L., Robinson, C. R., Zang, S. N. et al, 1999, *ApJ*, 517, 951
 Miller-Jones, J. C. A., Blundell, K. M., et al. 2004, *ApJ*, 600, 368
 Mioduszewski, A. J., Rupen, M. P., Hjellming, R. M., et al. 2001, *ApJ*, 553, 766
 Mirabel, I. F., Rodríguez, L. F., Cordier, B., et al, 1992, *Nature*, 358, 215
 Pandey, M. D., Durouchoux, P., Manchanda, R., et al, 2004, *Proceedings of 5th Integral workshop*, ESA
 Persi, P., Ferrari-Toniolo, M., Grasdalen, G. L., et al, 1980, *A&A*, 92, 238
 Pooley, G., Brocksopp, C., Fender, R. P., et al., 1999, *MNRAS*, 309, 1063
 Predehl, P., Wilms, J., Nowak, M. A., et al., 2002, *Proceedings of the 3rd Micro-quasar workshop*, ed. A.J. Castro-Tirado, J. Greiner, J.M. Paredes, (Dordrecht: Kluwer), 41
 Rickett, B.J., *ARA&A* 28, 561
 Rybicki, G., Lightman, A., 1979. 'Radiative processes in Astrophysics' (New York: Wiley)
 Rickett, B. J., Coles, W. A., Bourgois, G., 1984, *A&A*, 134, 390
 Rodríguez, L., Mirabel, F., Martí, J., 1992, *ApJ*, 544, 443
 Schalinski, C. J., Johnston, K. J., Witzel, A., et al. 1998, *A&A*, 329, 504
 Stirling, A., Spencer, R., de la Force, C., 2001, *MNRAS*, 327, 1273
 Stinebring, D.R., Smirnova, T.V., Hankins, T. et al. 2000, *ApJ*, 539
 van der Klis, M., Janson, F. A., 1985, *Nature*, 313, 768
 van Kerkwijk, M. H., Gebelle, T. R., King, D. L. et al., 1996, *A&A*, 314,521
 Waltman, E. B., Fiedler, R. L., Johnston, K. L. et al., 1994, *AJ*, 108, 179
 Waltman, E. B., Ghigo, F. D., Johnston, K. J., 1995, *AJ*, 110, 290
 Watanabe, H., Kitamoto, S, Miyamoto, S. et al : 1994, *ApJ*, 433, 350
 Wilkinson, P. N., Narayan, R., Spencer, R. E., 1994, *MNRAS*, 269, 67